

Improving Fractional Bandwidth and Isolation Between Tx and Rx Antennas Using EBGs at X-band

Nafis Hasnayan¹, Mehrab Ramzan¹, Swad Al Nahiyani¹, Padmanava Sen¹,

¹Barkhausen Institut, Dresden, Germany

{¹{nafis.hasnayan, mehrab.ramzan, swad.nahiyani, padmanava.sen}@barkhauseninstitut.org,

Abstract— In integrated sensing and communication (ISAC) applications, it is essential to have wide bandwidth and high isolation between transmitting (Tx) and receiving (Rx) antennas considering a full-duplex system. This paper demonstrates improved bandwidth and wideband isolation by employing sub-wavelength passive periodic structures, namely electromagnetic bandgap (EBG) structures at 10 GHz. The fabricated design exhibits a measured bandwidth of 1.89 GHz and a minimum isolation of around 42.4 dB at $0.5 \lambda_0$ separation distance between antennas with the help of the EBG structures. The proposed method can be used as a wideband isolation solution for X-band applications maintaining a small package size. In addition to this, this technique doesn't require active circuits and provides a cost-effective substitute for future 6G ISAC applications.

Keywords— Bandwidth, coupling, EBG, electromagnetic, isolation.

I. INTRODUCTION

Technology has allowed wireless communications and radar sensing to develop in parallel over the last decades. At the moment, radar and wireless communication systems are usually developed and implemented separately, using different hardware, waveforms, and specific areas of the radio spectrum [1]. Whereas radar systems are responsible for sensing and object detection, wireless communication systems focus on data transmission. Each of them has its frequency bands and its own infrastructure, which often results in inefficient use of the spectrum and resources. Integrated sensing and communication (ISAC) form a unique and efficient solution to use the same radio spectrum, hardware, and signal processing techniques to simultaneously provide both high-speed data transmission (communication) and environment sensing (radar).

In the near future, communication systems are likely to be deployed based on the in-band full duplex concept because of the demand for high data throughput and spectral efficiency [2]. Most automotive radar systems today, such as Frequency-Modulated Continuous Wave (FMCW) radars, use separate antennas for transmitting and receiving signals. In contrast to the half-duplex systems, a system designed according to the full-duplex principle do not require separate transmitter and receiver units. Antenna design has a significant role in full duplex systems because the same antenna needs to be operated both as a transmitter and a receiver. As a result,

it needs an advanced technique for self-interference handling and robust isolation.

The most common approach to achieve isolation in full-duplex systems is to maintain sufficient separation between the two antennas [3]. However, this significantly increases the size of the package and hence does not fit compact and high-frequency applications such as 6G and ISAC. The other common method includes the use of circulators; these usually bring additional complexity and are power-hungry-critical drawbacks for energy-efficient designs. EBG structures are already gaining popularity in terms of their capability to provide isolation in a full duplex system. EBG structures provide surface wave suppression that can enhance isolation while minimizing undesired mutual coupling between antennas.

The issues pertaining to mutual coupling have already been discussed in various literature [4][5][6]. Maintaining a wide bandwidth and good isolation simultaneously between the Tx and Rx modules is considered as one of the main challenges in the upcoming full duplex ISAC systems. This work discusses a solution to this dual addressed challenge using the passive EBG meta-surfaces. This work is an extension of our prior research demonstrated the utilization of EBGs for only reducing the coupling between Tx and Rx antennas at 26GHz [7]. In this paper, the concepts are applied at 10 GHz and the broader dual role of EBGs in coupling reduction and bandwidth enhancement is highlighted. The results are discussed in terms of different integrated configuration of EBGs and the improvement are highlighted in terms of bandwidth, coupling, gain and radiation efficiency of the integrated antennas.

The paper is presented as follows: Section II gives the theoretical background of the EBG unit cell; Section III presents the simulation and measured results of the integrated Tx and Rx antennas with EBG structures. Finally, the conclusion and future work of this research are discussed.

II. EBG UNIT CELL

Electronic Band Gap (EBG) structures are quite popular in the field of metamaterials and artificial materials. In recent time, their use has increased as they can achieve unnatural properties not available in nature. A widely accepted definition of EBG is "artificial and periodic (or non periodic) objects that prevent/assist the propagation of electromagnetic waves

in a specified band of frequency for all incident angles and all polarization" [8]. The application of EBG targeted in this paper is to increase the isolation between the Tx and Rx antennas by suppressing the surface wave. Surface waves are a common phenomenon in antenna and antenna array design. They are the waves that propagate along the interface of two materials and decay exponentially as they move away from the surface [9]. Because of the surface wave, the gain and efficiency of the antenna are reduced. In antenna array design the surface waves increase the mutual coupling. When EBG structures encounter surface waves as incident waves it shows a frequency band gap and prevents the surface wave from propagating for any incident angle and polarization. So a properly designed EBG structure accumulated with an antenna array can increase the isolation and reduce the mutual coupling.

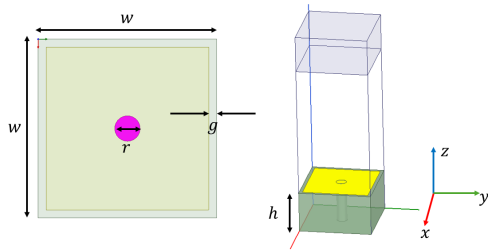


Fig. 1. EBG unit cell.

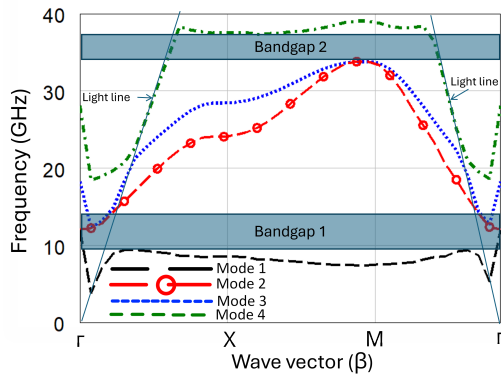


Fig. 2. Electromagnetic bandgap response of the mushroom structure optimized at 10 GHz.

The design of an EBG unit cell can be represented by an equivalent parallel LC circuit, where the resonance behavior is governed by the relationship between inductance and capacitance. The resonance frequency ω_0 of the unit cell is defined by the equation:

$$\omega_0 = \frac{1}{\sqrt{LC}}, \quad (1)$$

where L represents the inductance and C represents the capacitance of the equivalent circuit. To achieve a desired resonance frequency, the appropriate values of L and C must

be calculated based on the unit cell's geometric and material properties.

The inductance L is typically derived from the thickness of the substrate material and can be expressed as:

$$L = \mu_0 h, \quad (2)$$

where μ_0 is the permeability of free space, and h is the thickness of the substrate. The corresponding capacitance C can then be determined from the resonance frequency using the relationship:

$$C = \frac{1}{\omega_0^2 L}. \quad (3)$$

The physical dimensions of the unit cell, particularly the patch width w , are crucial for determining the capacitance. The capacitance C is related to the patch width by the equation:

$$C = \frac{w \varepsilon_0 (1 + \varepsilon_r)}{\pi} \cosh^{-1} \left(\frac{w + g}{g} \right), \quad (4)$$

where ε_0 is the permittivity of free space, ε_r is the relative permittivity of the substrate, g is the gap between adjacent patches and $g + w$ is the periodicity of the structure. The patch width w can be determined by solving this equation, ensuring that $g < w \ll \lambda$ for proper operation within the intended frequency band.

Based on these concepts, an EBG unit cell is designed and optimized accordingly to get the desired properties in the expected frequency of 10 GHz in the X band. All the parameters of the unit cell are mentioned in Table 1

Table 1. Dimensions of the Tx and Rx antenna board with EBG structures

Parameters	Values (mm)	Values (λ_0)	Values (λ_g)
L_s	29.94	0.998	1.919
W_s	51.51	1.717	3.302
L_p	7	0.233	0.4488
W_p	9.128	0.304	0.585
L_f	12.8	0.426	0.802
W_f	2.84	0.0946	0.182
L_t	4.344	0.1448	0.2785
W_t	1.3	0.0433	0.0833
S_p	15	0.5	0.9617
w	2.8	0.0933	0.1795
g	0.2	0.0066	0.01282
r	0.4	0.0133	0.02565
h	1.55	0.0516	0.0994
ε_r	3.7	-	-

The unit cell structure and the dispersion diagram of the EBG unit cell are depicted in Fig. 1 and Fig. 2. This dispersion diagram is used to understand how waves propagate through the EBG structure at different frequencies and wave vectors. When a mode exists, waves can propagate through the material at that frequency and wave vector. The different modes might correspond to different types of wave propagation, such as transverse electric (TE) or transverse magnetic (TM) modes, or they could be higher-order modes of the same type. The absence of modes in certain frequency ranges indicates

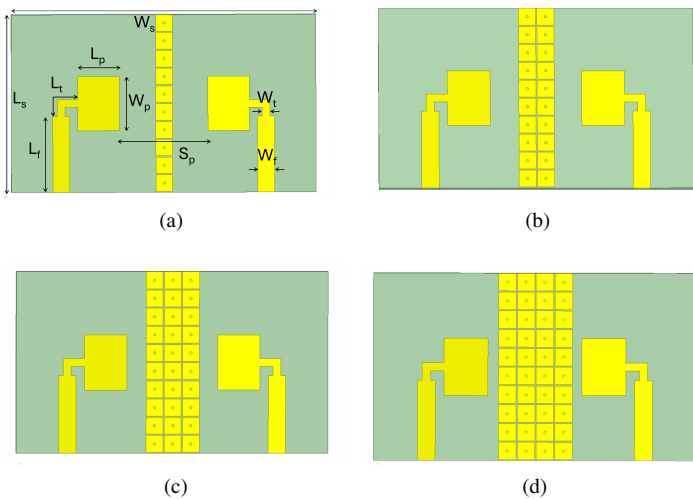


Fig. 3. Different configurations of EBGs: (a) antenna 1; (b) antenna 2 (c) antenna 3 (d) antenna 4.

band gaps, where no wave propagation is allowed. From the dispersion diagram, it is visible that around 10 GHz no mode exists. This means the EBG structure can suppress surface waves at 10 GHz for a wide range of wave vectors.

III. SIMULATED AND MEASURED RESULTS

In order to assess the different behavior of EBG integration on the antenna's reflection and transmission coefficient, it is divided into different designs, as shown in Fig. 3. The separation between the Tx and Rx antenna is kept fixed and different arrays of EBG structures are used and the design response is recorded during the EM simulations. For proof of concept, a cheap substrate based on FR4 substrate with permittivity of 3.7 and loss tangent of 0.025 is utilized. The impact of different configurations of the EBG on the reflection coefficient of the antenna is shown in Fig. 4. It is observed that 1×10 and 2×10 array have almost same impact on the reflection coefficient of the antenna and no significant bandwidth improvement is observed. As the EBGs are spread near the antennas, the Tx antenna starts showing a bandwidth increment. A significant improvement in bandwidth is observed with a 4×10 EBG array configuration, as shown in Fig. 4. It highlights the ability of EBG structures to enhance the antenna's bandwidth when placed in close proximity to the radiating antenna.

On the other side, the different designs transmission coefficient response is also recorded to evaluate the isolation improvement of the different EBG configuration. The antenna 1 and antenna 2 show an isolation level of approximately 20 dB in the entire frequency band, as shown in Fig. 5. As the EBGs start getting closer the antennas, the isolation starts improving and an isolation of 30 dB was observed when EBGs are kept in the near vicinity of the antenna as shown in Fig. 5. This demonstrates the simultaneous improvement of the bandwidth and isolation over a bandwidth of 1.89 GHz.

The fabricated antenna on FR4 substrates with the EBG structures is depicted in Fig. 6. The comparison of

measured and simulated results is provided in Fig. 7. The integrated antenna shows a wideband reflection coefficient behavior during the measurement. Moreover, the transmission coefficient results show better isolation values of more than 34 dB in the operating frequency bandwidth of 1.5 GHz. The improved results could be traced to the twisted wires used during the fabrication of the board for the shortening vias.

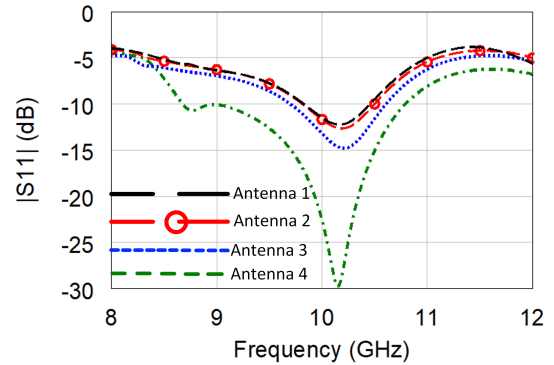


Fig. 4. Simulated reflection coefficient of Tx and Rx board with different EBG configurations.

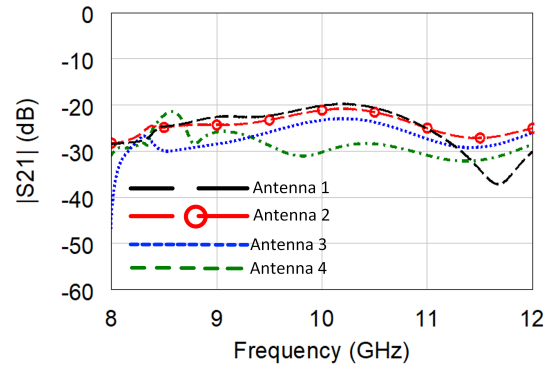


Fig. 5. Simulated transmission coefficient of Tx and Rx board with different EBG configurations.

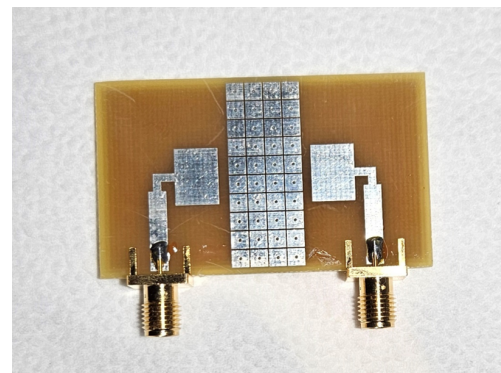


Fig. 6. Fabricated Tx and Rx board with EBG structures on a FR4 substrate.

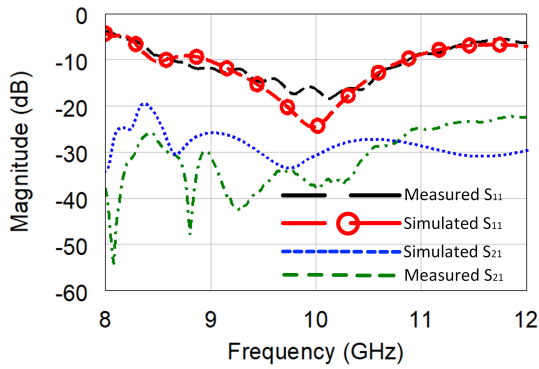


Fig. 7. Simulated and measured reflection and transmission coefficient of Tx and Rx board with EBG structures.

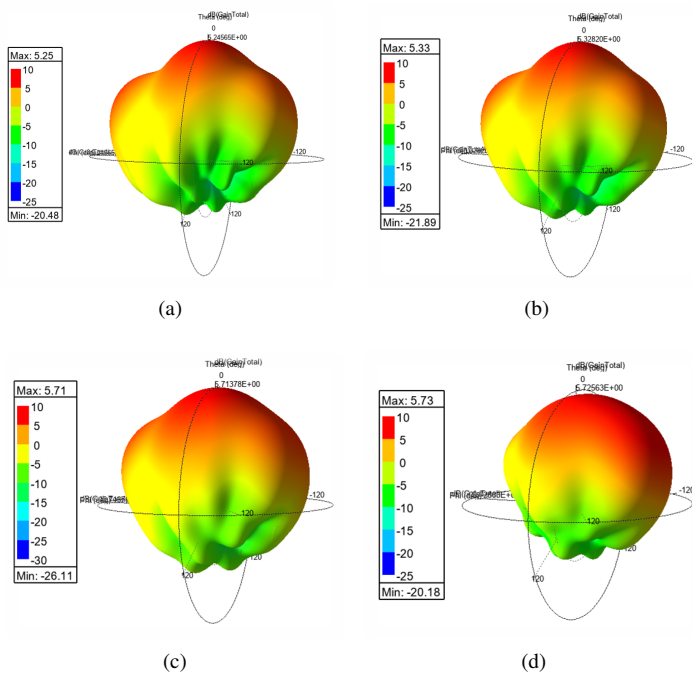


Fig. 8. 3D realized gain of EBG antennas: (a) antenna 1; (b) antenna 2 (c) antenna 3 (d) antenna 4.

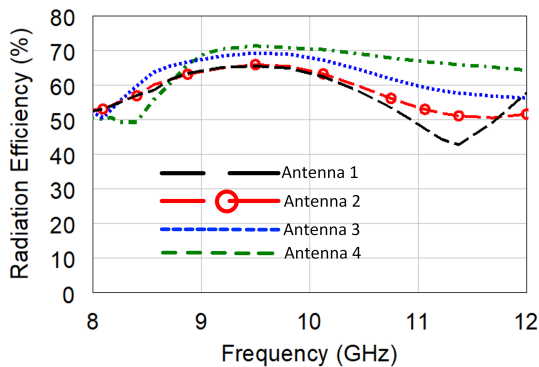


Fig. 9. Radiation efficiency of the antenna with respect to different EBG configurations.

The 3D realized gain of the antenna is also analyzed with respect to different designs, as illustrated in Fig. 8. Despite the presence of the EBGs in the near vicinity of the antennas, the Tx antenna showed a minimum gain of 5.24 dBi (antenna 1) and maximum gain of 5.73 dBi (antenna 4). The gain is influenced on the EBG side during the integration process, overall, the gain pattern shows acceptable radiating behavior as shown in Fig. 8 (d). Furthermore, the radiation efficiency of the different designs is also evaluated, as shown in Fig. 9. The results clearly indicate that integrating EBG structures at each stage improves the radiation efficiency of the antenna.

IV. CONCLUSION

In this work, the dual role of EBG structures to simultaneously improve isolation and fractional bandwidth is proposed. The near field coupling of the EBGs can be used to enhance bandwidth and reduce the coupling of the integrated antennas on a cheap substrate with a achieved average isolation of 34 dB and bandwidth of 1.89 GHz in the X-band. The bandwidth and isolation requirements in the integrated sensing and communication make this approach more attractive. Moreover, as a future work, the antennas will be integrated with a practical 6G demonstrator for validating its feasibility for the next-generation applications.

ACKNOWLEDGMENT

This work is funded by the German Federal Ministry of Education and Research under the KOMSENS-6G project with the grant number 16KISK122. The responsibility for the content of this publication lies with the author. This work is financed on the basis of the budget passed by the Saxon State Parliament.

REFERENCES

- [1] Z. Feng, Z. Fang, Z. Wei, X. Chen, Z. Quan, and D. Ji, "Joint radar and communication: A survey," *China Communications*, vol. 17, no. 1, pp. 1–27, 2020. DOI: 10.23919/JCC.2020.01.001.
- [2] J. Zhou, N. Reiskarimian, J. Diakonikolas, et al., "Integrated full duplex radars," *IEEE Communications Magazine*, vol. 55, no. 4, pp. 142–151, 2017. DOI: 10.1109/MCOM.2017.1600583.
- [3] M. Duarte and A. Sabharwal, "Full-duplex wireless communications using off-the-shelf radios: Feasibility and first results," in *2010 Conference Record of the Forty Fourth Asilomar Conference on Signals, Systems and Computers*, 2010, pp. 1558–1562. DOI: 10.1109/ACSSC.2010.5757799.
- [4] C. A. Balanis, *Antenna Theory: Analysis and Design*, 3rd. Hoboken, USA: Wiley, 2005.
- [5] D. Pozar, "Input impedance and mutual coupling of rectangular microstrip antennas," *IEEE Transactions on Antennas and Propagation*, vol. 30, no. 6, pp. 1191–1196, 1982. DOI: 10.1109/TAP.1982.1142934.
- [6] T. S. Bird, "Basics of antenna mutual coupling," in *Mutual Coupling Between Antennas*. 2021, pp. 9–26. DOI: 10.1002/9781119565048.ch2.
- [7] M. Ramzan, A. N. Barreto, and P. Sen, "Meta-surface boosted antenna to achieve higher than 50 db trx isolation at 26 ghz for joint communication and radar sensing (jc&rs)," in *2022 16th European Conference on Antennas and Propagation (EuCAP)*, 2022, pp. 1–5.
- [8] Y. Rahmat-Samii, "Electromagnetic band gap (ebg) structures in antenna engineering: From fundamentals to recent advances," in *2008 Asia-Pacific Microwave Conference*, 2008, pp. 1–2. DOI: 10.1109/APMC.2008.4958195.
- [9] M. Yaqoob, A. Ghaffar, M. A. Alkanhal, M. Naz, A. H. Alqahtani, and Y. Khan, "Electromagnetic surface waves supported by a resistive metasurface-covered metamaterial structure," *Scientific Reports*, vol. 10, no. 1, p. 15 548, 2020.